Spectroscopic assessment of the UV laser removal of varnishes from painted surfaces

Daniele Ciofini[(1)], Mohamed Oujja[(2)], Maria Vega Cañamares[(3)] Salvatore Siano[(1)] and Marta Castillejo[(2)]

(1) Istituto di Fisica Applicata ''N. Carrara'', CNR, Via Madonna del Piano 10, 50019, Sesto Fiorentino, Italy. email:d.ciofini@ifac.cnr.it
(2) Instituto de Química Física Rocasolano, CSIC, Serrano 119, 28006 Madrid, Spain.
(3) Instituto de Estructura de la Materia, CSIC, Serrano 121, 28006 Madrid, Spain.

Abstract

In the present work we focus on the assessment of the chemical and physical side effects induced by UV laser ablation of varnish samples (i.e. mastic, oil mastic, dammar and bleached shellac) after natural curing and artificial ageing using micro-Raman spectroscopy, laser induced fluorescence and environmental scanning electron microscopy. The varnish films were irradiated with the fifth (213 nm) and fourth (266 nm) harmonics of a Q-switched Nd: YAG laser. Besides the systematic microscopy inspection of the irradiated areas, a significant effort was devoted to the study of the optical properties of the varnish films by means of UV-Vis absorption spectroscopy, which allowed the determination of linear absorption coefficients at the present laser irradiation wavelengths. Single-pulse laser ablation thresholds were measured by applying the spot regression method and processing of the films was carried out using three different scanning speeds that resulted in 1, 5 and 10 laser pulses on each irradiated area. The results achieved using laser fluences well above the single-pulse ablation threshold of the treated varnishes, indicated the quality of the material removal process crucially depend on the irradiation wavelength, type of varnish and on its degree of polymerization. In contrast with the undesired modifications observed at 266 nm, that led to the formation of microbubbles, which produced a whitish appearance of the irradiated area, the absence of relevant side effect at 213 nm emphasizes the importance of using a highly absorbed wavelength to finely remove the altered uppermost layer of different types of aged varnishes.

Keywords: laser, ablation, varnish, terpenoid, Raman, LIF

1 Introduction

The removal/thinning of aged varnish coatings from easel paintings is a very complex issue since ageing and degradation phenomena strongly affect their chemical and physical properties, thus making difficult any restoration attempt. For instance, auto-oxidation through chain radical reactions, which occurs both in light and darkness according to different kinetics, is the most recognized degradation pathway [1]. Well-known macroscopic effects of ageing are: cracking, hazing, loss of gloss, yellowing and darkening over time, which produce significant aesthetic changes of the paintings. Studies carried out on mastic and dammar varnishes have also showed that owing to light and oxygen most of the oxidized and condensed products (i.e. carboxylic acids, esters, anyhydrides, lactones), also including high molecular weight compounds (i.e. quinones), are mainly generated in the uppermost varnish layer (within the first 10 μm) [2]. It is therefore expected that upon ageing, the

reduced number of cross-links and UV chromophores across depth will lead to changes in solubility and laser interaction properties [3, 4], which have a significant importance in conservation treatments. The latter need to be carefully optimized in order to recover the complete legibility of the painting and avoid any injuries to the remaining varnish film and the pictorial layers underneath. To this goals, presently the attention is strongly focused on the laser ablation approach, which is well-established in conservation of stone and metal artefacts, as well as wall paintings [5-7] and in principle could satisfy the mentioned requirements if the irradiation parameters are carefully optimized, but further investigation are needed.

Since the early eighties, many laser systems operating in different spectral regions and pulse durations have been proposed for restoration of paintings. Nanosecond (20-50 ns) excimer lasers emitting at 351 nm (XeF*), 308 nm (XeCl*), 248 nm (KrF*), and 193 nm (ArF*) [8-15], Free Running (200-400 μs) Er:YAG (2.94 μm) laser [16], Q-Switched (5-15 ns) and Long Q-Switched (60-120 ns) Nd:YAG lasers (1064, 532, 355, 266, 213 nm) [17-23] have been used in laboratory tests aimed at assessing the laser-induced effects on pigments, binders, varnishes and their mixtures.

Furthermore, recently LQS Nd: YAG laser has also been successfully used for the first time in a practical overpaint removal from a modern oil painting on canvas [24].

In previous studies, the most used wavelength for thinning aged varnish coatings has been 248 nm (KrF* laser) [25], although a much better surface morphology and in-depth control was achieved using 193 nm [9-10] (ArF* laser). On the other hand, the higher ablation rates observed at 248 nm are better suited for achieving sufficient etching across the typical varnish layers found in paintings. The mean ablation rates of different types of spirit and oil varnishes (i.e. dammar, mastic, copal-oil and shellac) is between 0.5-1 μm/pulse in a fluence range of 0.2-0.6 J/cm^2. However, the large sizes, weight, complex maintenance, and safety issues of the excimer lasers make them not suitable for widespread use in the present application field. Thus, according to the general trend observed in laser material processing, where gas lasers are being gradually replaced by solid state sources, the previous results represent the starting point for exploring the potential of the most advanced UV solid state lasers.

Recently, with the aim of minimizing photo-thermal, photo-mechanical and photo-chemical undesired effects, ultra-short lasers operating in picosecond (ps) and femtosecond (fs) regimes have been tested [26-27]. Processing of fresh mastic and dammar varnishes with 248 nm, 500 fs laser pulses resulted in an improved etched morphology as compared with ns pulses at the same wavelength [26]. Simultaneously, encouraging results were achieved using the fifth harmonic of a QS Nd: YAG laser (213 nm, 15 ns) nm, which allowed micrometric gradual removal of shellac from photo-sensitive tempera paint models without affecting the surface morphology and chemical composition of the remaining varnish film and underlying paint layers. In contrast, fs multiple pulse Ti:Sapphire irradiation at 795, 398 and 265 nm has turned out to be ineffective for removing shellac varnish from egg-yolk based tempera paints [27].

Here, we extend this early investigation by focusing on the assessment of undesired chemical and physical modifications of various natural resin varnishes typically encountered in conservation of easel paintings. Furthermore, besides the fifth (213 nm) also the fourth (266 nm) harmonic of the QS Nd: YAG laser was comparatively tested in order to thoroughly explore the potential of this laser source in selective removal of aged varnishes. To this goal, laser induced-effects on naturally cured and artificially aged samples of solvent mastic, dammar and bleached shellac varnishes along with oil mastic varnish, were thoroughly investigated by using micro-Raman spectroscopy, laser induced fluorescence and environmental scanning electron microscopy (ESEM).

2 Material and methods

2.1 Laboratory samples

Varnish samples were prepared according to the following methodology. Dammar, "Chios" mastic and light shellac (bleached) (marketed by Zecchi, Florence) pure resins were dissolved in a suitable solvent (30% w/v) which was white spirit, iso-propanol and ethanol, respectively. Mastic-oil varnish was prepared by heating oil and resin up to 220 °C using a sand bath. The mixture was allowed to cool slowly until 60 °C when rectified turpentine oil in 1:1 wt% was added to the oil-resin mixture. Afterwards, varnish films were applied by casting on synthetic round quartz plates (2.5 cm diameter, 2.5 mm thick) and eventually finely brushed on primed canvas. The latter was constituted of a commercial blend of calcium sulphate and calcium carbonate, bound with a proteinaceous binder, which represents a weakly absorbent ground suitable for paintings.

A set of reference samples, was left cured for about 20 months in controlled laboratory conditions (T= 20 °C, R.H= 40-45%) behind a glass-window and protected from dust and the direct sunlight radiation (i.e. the reference samples). A second set of samples was artificially aged in an air-cooled Xenon test chamber (500 hours, B.S.T= 50°C, cut-off of 290 nm, 50 mW/cm^2). Once artificial ageing was completed, the samples were exposed to free oxygen conditions for 6 months and then stored in the dark for about one year prior to be investigated.

2.2 UV-Vis absorption spectroscopy

UV-Vis absorption spectra were collected using a Shimadzu UV3600 double-beam spectrophotometer. The spectral window was settled in a wavelength range of 200-800 nm with a sampling interval of 1 nm and a scan speed of 200 nm min^{-1}. Dedicated samples were suitably prepared on quartz plates as thin films in order to correctly measure the UV-Vis absorption. For this reason, a small amount (of the order of mg) of each varnish film was weighted in a Sartorius Research balance with a readability of 10^{-5} g. The weighted amount was grinded and then dissolved in equal concentration of about 0.086 % (0.00259 g/3cc) (weight to volume) by selecting a suitable solvent or blend by Teas chart (see Table 1) [28].

An ultrasonic bath was used to speed up the dissolution process. Afterward, a volume of about 3 ml was cast by graduated Gilson micropipette on round quartz plates (5 cm diameter, 2 mm thick). Once the films were dried and the solvent completely evaporated, the resulting thickness was measured using a Digital Comparator (Mahr Extramess) with a resolution of up to 0.2 µm. The measured values ranged between 1.5-2 µm. The spectra collected covered an absorbance range, which was well-below the spectrophotometer saturation threshold of 3 absorbance units. All the spectra reported below were achieved by plotting the mean absorption coefficient (α_{mean}) as a function of wavelength and no solvent subtraction was needed in order to correct the absorption profiles. α_{ref} and α_{aa}, as reported in section 3.1.1, correspond to the absorption coefficient of reference and artificially aged samples, respectively.

First order derivatives were calculated over the whole spectral window in order to find the correct position of the inflection point, which provides useful information about the wavelength of maximum absorbance. Afterwards a slight (5 points) average-adjacent smoothing filtering was applied in order to improve the signal-to-noise ratio.

2.3 Micro-Raman spectroscopy

Micro-Raman analyses were performed on the varnish films applied on round quartz plates in order to study both the material photo-degradation processes and the laser-induced modifications. Micro-Raman spectra were recorded using a 785 nm excitation wavelength Renishaw System coupled to an optical microscope. The Raman signal was calibrated using the emission line at 520 nm of a standard Si target. The grating was 1200 lines/mm and the spectral resolution about 2 cm^{-1}. The excitation laser was focused onto the sample surface using a 50x (NA 0.55) objective lens allowing for a spatial (lateral) resolution down to 1 µm. The spectra collected are presented without any correction.

2.4 Laser Induced Fluorescence spectroscopy

Laser Induced Fluorescence (LIF) measurements were performed on reference and artificially aged varnish films applied on primed canvas using an excitation wavelength of 266 nm, which is a sensitive probe for assessing the laser-induced modifications. LIF spectra were measured using a 0.30 m spectrograph with a 300 lines mm^{-1} grating (TMc300 Bentham) coupled to an intensified charged coupled detector (2151 Andor Technologies) providing a spectral coverage of 280 nm. The spectral range was centered around 450-500 nm and a 320 nm cut-off filter was used in order to reject the second order peak of emissions at lower wavelengths including the excitation one. The time gating was synchronized with the excitation laser pulse and had a duration of 3 µs.

The surface of the sample was illuminated at an incidence angle of 45° with a pulse energy less than 0.1 mJ and a spot of about 3 mm^2 (fluence of 3 mJ/cm^2). Each spectrum was the average of 20 measurements acquired in two different points of each irradiated area [27]. The selected repetition rate was 1 Hz. All the recorded spectra were normalized to their maxima to be independent from the incident intensity and the quantity of analyzed material.

2.5 Microscopy examination

Micro-morphological changes of the laser irradiated films were preliminary investigated via optical microscope examination (Leica DM LM microscope) and Raman microscopy (RM). Closer inspections were carried out using an environmental electron microscope (ESEM, Quanta-200 FEI) mainly exploiting back scattered electron (BSE) scans and using acceleration voltage of 25 kV and pressure of 1 Torr.

2.6 Laser ablation thresholds

Laser irradiation tests were performed using a QS Nd: YAG laser (Lotis II, LS-2147) operating at the 4th (266 nm) and 5th (213 nm) harmonics with a pulse duration of 15 ns and a repetition rate of 1 Hz. The average pulse-to-pulse energy fluctuations were of about 10 % for both the harmonics. The laser beam was focused on the surface of the sample by means of a spherical plano-convex quartz lens with focal length of 80 mm at a fixed distance of about 71 mm. For continuous control of the laser pulse energy, a suitable variable dielectric attenuator (Laser Optik) was used.

Ablation fluence thresholds were determined by measuring the minimum pulse energy at which gas desorption was observed and calculating the size of the irradiated area by applying the spot regression method using a sensitive photographic film [27, 29, 30].

For laser beams with a Gaussian spatial profile, the maximum laser fluence, F, on the sample surface and the diameter, D, of the ablated area are related by $D^2=2\omega_0^2\ln (F/F_{th})$, where ω_0 is the $1/e^2$ radius of the Gaussian beam distribution and F_{th} is the ablation fluence threshold. The diameter of the ablated area was determined as observed on the photographic film through optical microscopy. From a plot of D^2 versus lnE, E being the pulse energy, F_{th} and ω_0 can be determined. The value of ω_0 was calculated by a linear fit, taking the slope as equal to $2\omega_0^2$. The calculated values of ω_0 were 0.3 and 0.55 mm at 213 and 266 nm respectively.

2.7 Laser processing

Laser ablation tests of the various varnishes were carried out at the two irradiation wavelengths on quartz and canvas substrates. Each varnish sample was processed at fluences two times higher than the corresponding to single-pulse ablation threshold ($2F_{th}$) previously measured. This value was chosen to maximize the ablation efficiency, in terms of ejected material per incident fluence unit.
The laser beam at both wavelengths was focused at the varnish surface using a cylindrical plano-convex quartz lens with focal length of 150 mm whose spot size was about 6.0x0.1 mm^2 at 213 nm and 5.5x0.1 mm^2 at 266 nm. Each area was processed at a repetition rate of 10 Hz following two different scanning procedures. The first one was achieved by manually turning a microstage over the entire scanned area and the second one using a motorized stage setting 0.1, 0.2 and 1 mm/s as scan-speeds along the x direction. The latter correspond respectively to 10, 5 and 1 laser pulses/step delivered for each laser spot. Using the n=1-l/2r, where n is the pulse overlap, l is the length between the center of two successive laser spots and r the spot radius (half width of the rectangular laser spot, r=0.05 mm), the pulse-overlap can be easily estimated. Considering the three scan speeds reported above the pulse overlap were 90%, 80%, and 0 %, respectively. Chemical and physical modifications upon laser removal at 213 and 266 nm were evaluated on scanned areas at 0.1 mm/s (10 laser pulses, overlap 90 %) with a fluence of $2F_{th}$.

3 RESULTS

3.1 Characterization of samples

3.1.1 UV-Vis light absorption spectroscopy

Figure 1 displays the spectral behaviours of the absorption coefficients and the corresponding first derivative of the varnish films understudy. The intense negative peaks at about 206 nm (α_{ref}=2400 cm^{-1}) and at 210 nm (α_{aa}=2500 cm^{-1}) refer to the inflection points of the first absorption maxima of reference and artificially aged mastic films (Fig. 1a), respectively. These peaks fall approximately at 190 nm, which is out of the spectrophotometer range. Furthermore, reference mastic films showed an evident shoulder at about 245 nm (α_{ref} =1000 cm^{-1}), which is barely observable in the first derivative of the artificially aged sample. In presence of linseed oil, the absorption pattern is slightly different with respect to pure mastic (Fig. 1b). The negative peaks are for both samples at 203 (α_{ref}=3000 cm^{-1}) and 204 nm (α_{aa}=2950 cm^{-1}). The shoulder-peak is here present at 230 nm, and, as previously discussed in mastic, the latter is more pronounced in the reference sample (α_{ref}=1450 cm^{-1}) than in the light aged one (α_{aa}= 1400 cm^{-1}).

Contrarily to mastic, the first derivative of dammar samples present the negative peak at about 205 nm (α_{ref}= 3850 cm^{-1} and α_{aa}=2800 cm^{-1}). The broad shoulder band centred at 235-240 nm (α_{ref}=1340 cm^{-1}) in the spectrum of reference dammar (Fig. 1d), which does not appear in the sample artificially aged, can be considered a real absorption maximum.
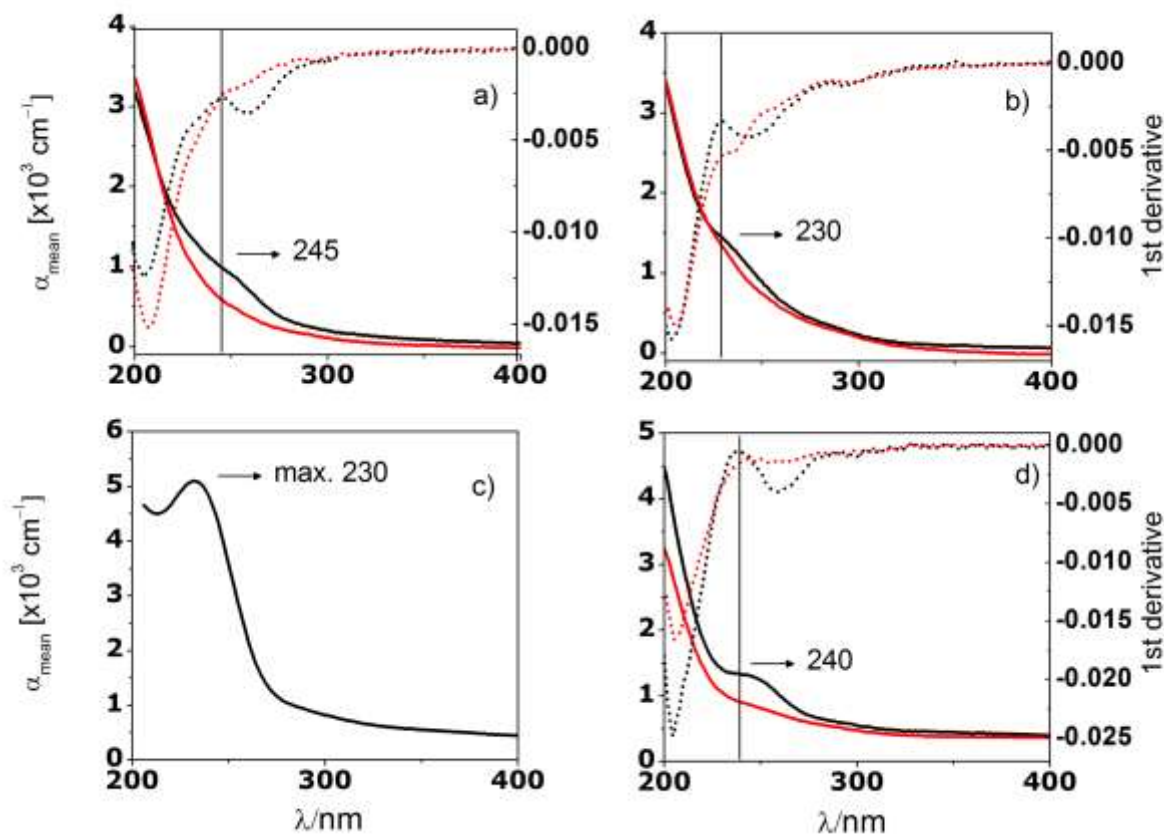

Figure 1 Mean absorption coefficients (solid lines) and their 1st derivatives (dotted lines) as a function of wavelength of non-irradiated mastic (a), mastic-oil (b), bleached shellac (c), and dammar (d) varnish samples. Black and red lines refer to reference and artificially aged samples.

The spectrum of reference bleached shellac (Fig. 1c) is characterized by a broad absorption peak with a maximum centred at about 230 nm (α_{ref}=5150 cm^{-1}). For this evident reason, no differentiation was applied. This maximum is assigned to α, β-olefinic carboxyl chromophore with a clear UV absorption in the 220-230 region [31, 32]. Specifically, epishellolic acid has a maximum at 226, jalaric acid at 220 and shelloic at 218 nm suggesting a carboxylic function conjugated with an olefinic linkage [33, 34]. Aleuritic acid is essentially transparent in the near UV region.
The artificially aged bleached shellac sample was not reported due to the complete loss of solubility in all the common organic solvents (see Table 1).

3.1.2 Characterization of samples by micro-Raman spectroscopy

Micro-Raman spectra recorded both on reference and artificially aged samples prior to the laser irradiation tests are shown in Fig. 2. This preliminary comparison allowed discriminating the structural differences among the studied terpenoid varnishes along with those induced by ageing.

In general, small changes are observed in the Raman spectra of varnishes during artificially ageing (Fig. 2). The most important changes are observed in the 1800-1500 cm^{-1} region, corresponding to C=O and C=C stretching vibrations and also in the 1300-700 cm^{-1}. A tentative assignment of the observed Raman bands is summarized in Table 3 [36-43].
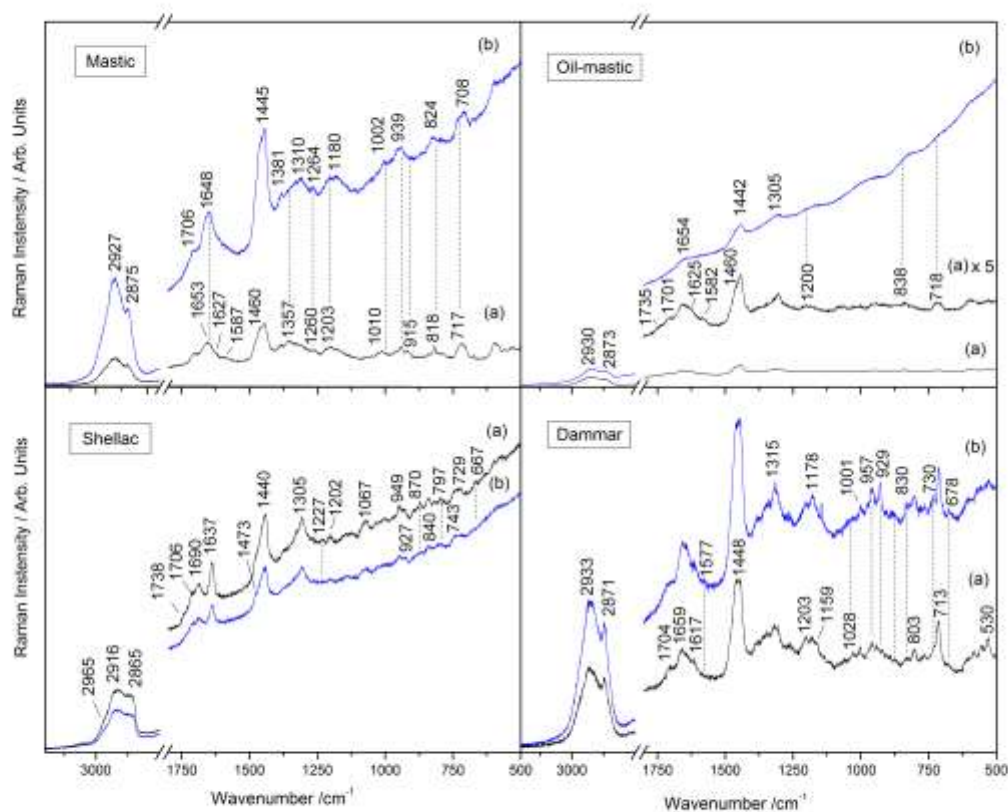

Figure 2. Micro-Raman spectra of (a) reference and (b) artificially aged mastic, oil mastic, shellac and dammar. The Raman spectrum of the reference oil-mastic sample was multiplied by 5 in order to show the low intensity bands of the spectrum.

In particular, in the case of mastic and oil-mastic Raman spectra, an increase of the fluorescence is observed upon artificial ageing. The most important changes in the mastic sample are small shifts of bands at 1653 to 1648 cm^{-1}, and the disappearance of the band at 1587 cm^{-1}. These modifications can be related to minute changes in the C=O bonds and to the disappearance of C=C bonds due to oxidation and cross-linking. On the other hand, the artificially ageing process lead to an increase of the bands at 1310, 1180, 1002, 952, 824 and 708 cm^{-1}. These bands are assigned to deformation vibrations of CH$_2$/CH$_3$, breathing of C-C rings, deformation of C-C ring, rocking of CH$_3$, stretching of C-C ring and out-of-plane deformation of C-H. The observed changes fit well with ring opening (Norrish type I reaction), fragmentation and oxidation of the triterpenoid skeleton [35]. The Raman spectrum of the reference sample of oil-mastic showed several differences with that of pure mastic (Fig. 2a). A weak band at 1735 cm^{-1} appears, related to the C=O bond of esters. Besides, the band at 1625 cm^{-1} is increased and that at 1587cm^{-1} in mastic is shifted to 1582 cm^{-1} in oil-mastic. These changes indicate the appearance of additional unsaturations and ester groups and may be, therefore,

7

related to polyunsaturated fatty acid chains (linseed oil) and monoterpenes (turpentine oil). The increase of the band at 1305 cm^{-1} in the Raman spectrum of oil-mastic, assigned to CH_2 in-plane twisting is ascribed to linseed oil. Other bands in the 1200-800 cm^{-1} almost disappear in the oil sample. This fact is even more evident in the artificially aged oil-mastic Raman spectrum. Other changes in the ageing process of the oil-mastic varnish are the disappearance of the bands at 1735 and 1582 cm^{-1}.

The Raman spectra of shellac undergo small changes after ageing, such as the disappearance of the bands at 1738, 1230, 870, 729 and 667 cm^{-1}. These bands are assigned to stretching of the C=O ester group, deformation of CCH, rocking of CH, stretching of CH and breathing of the C-C ring, respectively. Thus, little or no oxidation processes occurred in the ageing process. Changes on the C-C ring bands together with the disappearance of the band at 870 cm^{-1} depend on the fragmentation of the aliphatic chain, mostly present in aleuritic acid, a main component of shellac.

The ageing of dammar leads to several modifications on the Raman spectra of the varnish. Shifts of the bands at 1704 and 1659 cm^{-1} to 1707 and 1654 cm^{-1} in the artificially aged sample are related to changes in the C=O and C=C bonds. The same happens with the appearance of a band at 1577 cm^{-1} in the Raman spectrum of the aged sample. Increases of the intensity of bands at 1178, 957, 929, 830, 730 and 678 cm^{-1} are also observed. The first band cannot be assigned. The following two bands are related to rocking vibrations of CH_3. The band at 830 cm^{-1} corresponds to stretching of C-C-OH. That at 730 cm^{-1} is assigned to out-of-plane deformation of C-H. The last band, at 678 cm^{-1}, correspond to C-C ring breathing. A decrease of the bands at 584, 556 and 530 cm^{-1} is shown in the aged sample compared to the reference. This indicates further modifications of the C-C-O groups in the lateral substituents of oleanane and ursonic molecules. The changes observed are similar to that observed previously for mastic and may suggest also in this case ring opening reaction.

3.1.3 Characterization of samples by Laser Induced Fluorescence

LIF spectra recorded at the laser excitation wavelength of 266 nm on reference and artificially aged varnish samples are displayed in Fig.3. They were characterized by broad and unstructured bands with fluorescence maxima (λ_{max}) occurring at different emission wavelengths. In most cases, λ_{max} showed a slight bathochromic shift (red-shift) with ageing, evident in oil mastic, and a marked increase of intensity, mainly due to the formation of new chromophores (accumulation of unsaturated and oxidized products) in the outer varnish layer.

The fluorescence emission in mastic and dammar showed λ_{max} respectively at 475 (Full Width at Half Maximum, FWHM of 120 nm) and 459 nm (FWHM of 115 nm), which shifted 6 nm with ageing in both resins. As reported in the literature [44], the differences in the fluorescence of mastic and dammar have not yet been ascribed to specific fluorophores, although a significant contribution from α-pinene and β-myrcene polymeric fraction is expected. The $\Delta\lambda_{max}$ fluorescence shift of 13 nm between reference (λ_{max}=479 nm) and artificially aged (λ_{max}= 492 nm) oil-mastic samples may be related to the previous heating effect and to the greater photo-oxidative liability of fatty acid chains.

The LIF spectrum, recorded on reference bleached shellac, consists of a wide band with λ_{max} centered at 442 nm, which is, however, slightly narrower (FWHM of 100 nm) in comparison with those observed in triterpenoid resins. As expected, no evidence of bands at 355, 375, 495 and 630 nm assigned to fluorescent residual laccaic acids (orange-red fluorescence) were appreciated, although only a slight shoulder at about 490 nm (ascribed to hydroxy acids) is barely distinguishable [27-45].

A $\Delta\lambda_{max}$ fluorescence shift of 8 nm and a higher fluorescence intensity were observed and could be therefore associated to the ester linkages occurring during photo-induced polymerization.
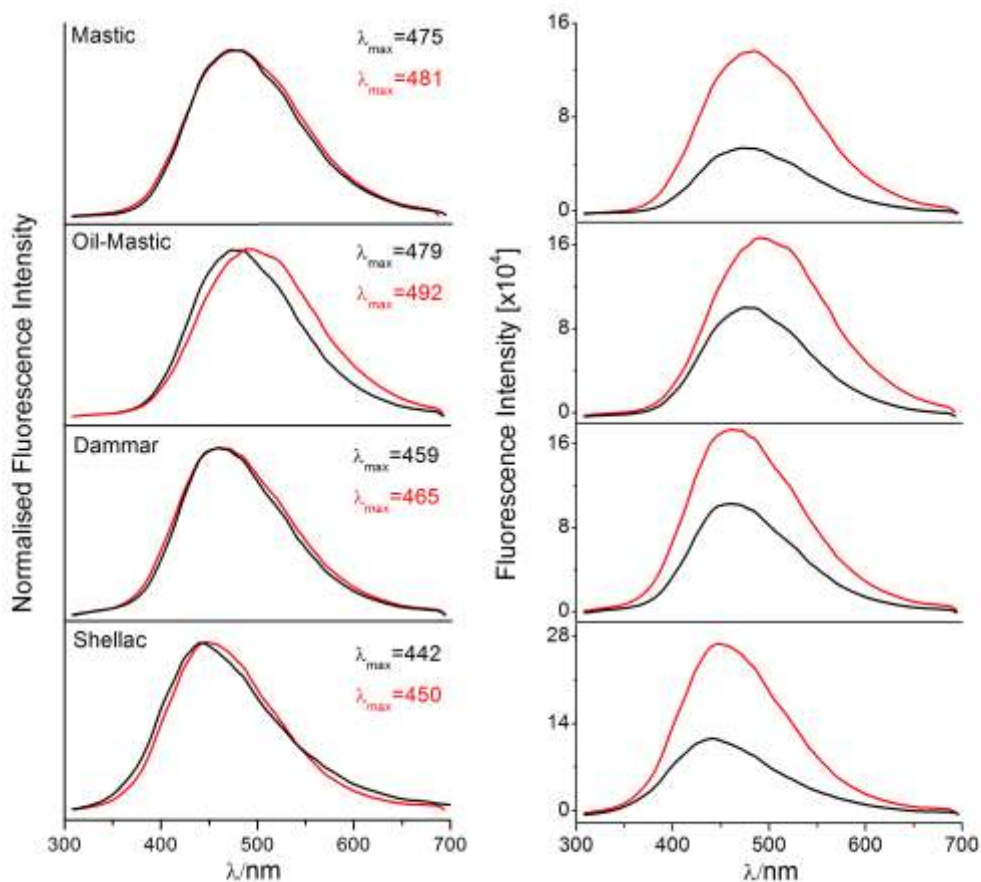

Figure 3. LIF spectra (exc. 266 nm) with (left) and without (right) fluorescence intensity normalization of reference (black line) and artificially aged (red line) varnish samples. λ_{max} refers to the maximum emission wavelength.

3.2 Laser irradiation

3.2.1 Ablation thresholds

Single-pulse ablation threshold fluences, F_{th}, were measured applying the spot regression method, as described in section 2.6. The decision on the onset of material removal (ablation threshold) was rather simple upon irradiation at 266 nm, thanks to the corresponding occurrence of a well-visible emission of gas from the irradiated area. This process was less pronounced at 213 nm, but it was still appreciable to the naked eye. The results obtained for all the varnishes are summarized in Table 2. For comparison purposes, the linear absorption coefficient (α) and the optical penetration depth ($\delta = 1/\alpha$), as derived from UV-Vis spectroscopy are also reported.

The operating fluence ranges for irradiation at 213 nm of reference and aged samples were similar, thus allowing, independently from their degradation, the processing of different terpenoid varnish types with only one wavelength. This feature, which is meaningful from the conservation standpoint, was not observed for irradiation at 266 nm. For the latter, F_{th} were very similar for mastic and dammar samples, while increased for oil-mastic and bleached shellac. Generally, the ratio F_{th} (266 nm)/F_{th}

9

(213 nm) varied between 3.7 and 6.4 thus indicating an evident higher absorption of the varnishes at 213 than at 266 nm. Similarly, α_{mean} (213 nm)/ α_{mean} (266 nm) ranged between 3.1 and 5.8, which is consistent with the previous F_{th} ratios. Furthermore, no remarkable differences were detected between F_{th} and α of reference and artificially aged samples, tough the latter exhibited mostly at 266 nm a lower α (higher δ), as pointed out also by UV-Vis absorption profiles (see 3.1.1).

Table 1. Single-pulse laser fluence thresholds, (F_{th}, mJ/cm^2), absorption coefficient (α, cm^{-1}) and optical penetration depth (δ, μm) measured on reference and artificially aged varnish films at 213 and 266 nm. The estimated error on F_{th} is less than 5 %, while for α can vary from 15 to 30 % depending from the solvent-extractable material (see **Error! Reference source not found.**, section 2.2).

Laser wavelength	213 nm			266 nm			ratios	
Description	F_{th} (mJ/cm^2)	α (cm^{-1}) x 10^3	δ (μm)	F_{th} (mJ/cm^2)	α (cm^{-1}) x 10^3	δ (μm)	F_{th} 266/213	α 213/266
Reference								
mastic	80±2	2.2	4.5	300±5	0.55	18.3	3.8	4.0
mastic-oil	90±3	2.1	4.8	455±8	0.55	18.3	5	3.8
dammar	85±3	2.6	3.9	315±6	0.85	11.8	3.7	3.1
shellac	85±2	4.6	2.1	530±9	1.25	7.9	6.4	3.7
Artificially aged								
mastic	70±2	2.2	4.5	275±5	0.38	26.3	3.9	5.8
mastic-oil	80±2	2.2	4.7	475±9	0.52	22.5	5.7	4.8
dammar	60±2	2.0	5.0	275±5	0.65	14.6	4.5	3.1
shellac	85±2	n.m*	--	520±9	n.m	--	6.3	n.m
*n.m : not measurable								

3.2.2 Laser processing

The varnish models were irradiated by scanning the laser beam over the sample surface using three different speeds (see section 2.7) corresponding to 1, 5, 10 delivered pulses/step at a fluence of 2 F_{th}. Particular care was devoted to safeguard a thin varnish film (5-10 μm) over the quartz and paint substrates, within which were then investigated the possible chemical changes (section 3.2.3 and 3.2.4). Previous RM inspections performed on the manually laser-scanned areas showed surface inhomogeneity in the scanning process, which were improved by using the motorized stage for moving the sample. However, none of the three speeds used served to return a flat surface morphology, most probably due to the partial synchronization between delivered laser pulses and motor steps and, the spatial energy fluctuations of the laser beam. Fig. 4 displays dark field images and back scattered electron (BSE) details of mastic and oil-mastic varnish samples after laser-scanning.

The areas irradiated at fluences well above the single-pulse ablation threshold (2F_{th}) were ablated and/or morphological modified, depending markedly on the irradiation wavelengths and degree of polymerization, but less from the type of varnish.

Irradiation at 213 nm induced ablation without noticeable morphological changes to the remaining varnish layer, which preserved its natural gloss (Fig.4a). A high resolution layer by layer removal was achieved. In particular, on reference mastic sample treated with a fluence of 2F_{th} and 10 successive laser pulses, an overall etched depth of about 4±0.5 μm was measured. This value, which

is 10 times lower than the optical penetration depth δ reported in section 3.2.1, has to be considered as averaged on a surface with a grating-like morphology. Irradiation at 266 nm gave rise to the nucleation of microsized bubbles, as shown in Fig. 4g-l. Bubbles of about 10-15 μm were observed also in dammar and shellac samples (data not shown). In this case, the average etch depth achieved on the reference mastic sample under the same irradiation conditions ($2F_{th}$, 10 pulses) was of 15±1.5 μm, which was 3.7 times larger than the thickness removed by irradiation at 213 nm. Most importantly, the remaining varnish layer, of the order of 5-10 μm, acquires a whitish and foamy appearance as result of an increased light scattering (Fig.4f).
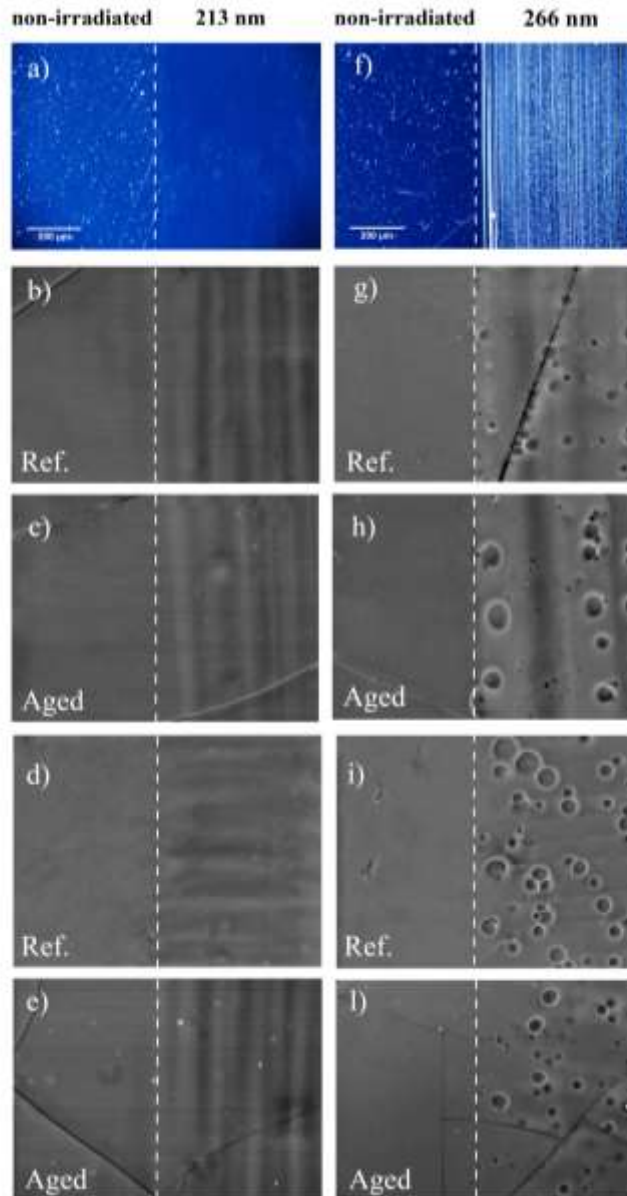

Figure 4 Fig. 4. Comparison between non-irradiated and laser irradiated areas at 213 (left column) and 266 nm (right column) with a fluence of $2F_{th}$ and 10 laser pulses/step (0.1 mm/s, overlap 90 %). Optical microscope images (a,f) taken on a varnish film applied on quartz substrate, which was in turn placed on a blue plastic film in order to make more evident the whitish appearance upon irradiation at 266 nm. BSE details show morphological changes induced in the

remaining oil-mastic (b,g,c,h) and mastic (d,i,e,f) varnish films. Ref. and Aged indicate reference and artificially aged samples, respectively. The size of each BSE picture is 165x140 μm.

3.2.3 Characterization of laser irradiation effects by micro-Raman spectroscopy

To assess the laser-induced chemical modifications on the remaining varnish layer and to investigate in depth the laser ablation process, a thorough characterization by using micro-Raman spectroscopy (exc. 785 nm) was carried out on laser treated (2 F$_{th}$, 10 pulses) areas.

Mastic, dammar and oil-mastic
Figure 5 displays micro-Raman spectra of mastic, oil-mastic and dammar varnish films acquired before and after laser irradiation at 213 (b) and 266 nm (c)**.** The Raman spectra of the reference mastic sample showed little differences after irradiation (Fig. 5A).
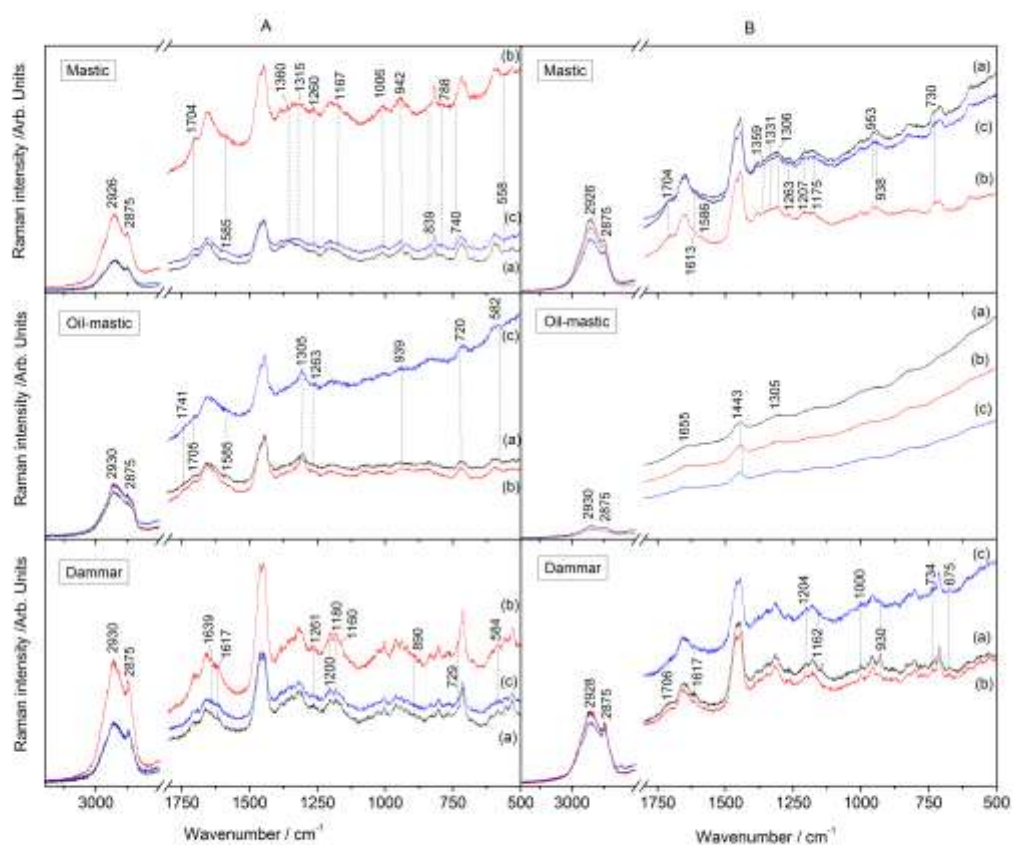

Figure 5 Micro-Raman spectra of reference (A) and artificially aged (B) samples of mastic, oil-mastic and dammar: non-irradiated (a), irradiated at 213 (b) and 266 nm (c).

An increase of the band at 1704 and a broadening of that at 1585 cm^{-1} were observed upon irradiation at 213 nm. The former band is assigned to the stretching of the C=O group and the latter to the C=C and CCH groups. Furthermore, an increase of the bands at 1315 and 1167 cm^{-1} were also observed,

12

which are associated to CH_2/CH_3 and C-C vibrations, respectively. On the other hand, irradiation at 266 nm led to a Raman spectrum apparently identical to that of the non-irradiated sample. Decrease of the bands at 1360 and 558 cm^{-1} were observed, which are related to deformations of the CH_2/CH_3 and of the C-C-O groups. The latter band got smaller also upon treatment at 266 nm.

Regarding the artificially aged samples (Fig. 5B) even less differences were found. As in the reference sample, an increase of the bands around 1600 cm^{-1} was observed after irradiation at 213 nm. Bands at 1263, 1207, 1175, 953 and 938 cm^{-1} were better defined in the (b) spectrum as compared to the (a) and (c). These bands correspond to vibrations of the deformations of CCH and =CH in-plane and rocking of CH_3, that could be related to polymerization processes. Finally, an increase of the band at 730 cm^{-1}, was observed as well. The irradiation treatment at 266 nm did not show significant differences in the spectra compared to the non-irradiated sample, although a decrease in the shoulders at 1704 cm^{-1} was clearly observable.

The laser treatments applied to the oil-mastic gave rise to very little variations among the Raman spectra. In the case of the reference samples (Fig. 5A) a small decrease of the bands at 1741, 1705 and 1585 cm^{-1} related to C=O and C=C was observed upon irradiation at 266 nm. These samples can be considered highly oxidized after the thermal treatment and curing procedures. Thus, at this wavelength the loss of the mention spectral features could be ascribed, as previously observed for pure mastic film, to an ablation mechanism driven by a photo-thermal process consisting in emission of small fragments and gaseous products (RCH_2OH, CH_3, CH_2, COOH, RCOOR, CO and CO_2).The comparison among the Raman spectra of the aged samples is quite difficult due to the low intensity of the bands. This probably happens because the photo-oxidative reactions took place throughout the film.

In the case of the dammar reference varnish samples, the Raman spectrum after irradiation at 213 nm showed an increase of the bands at 1639, 1200, 1180 and 1160 cm^{-1}. The first one is assigned to C=O and C=C vibrations and the other three to CCH and C-C. The irradiation at 266 nm led to a Raman spectrum apparently identical to that of the non-treated sample. The only differences are the light weakening of minor bands at 1261, 890 and 582 cm^{-1}. As in the previous varnishes, the artificially aged dammar samples showed less differences among the non-irradiated and irradiated Raman spectra, although C=O stretching at 1706 cm^{-1} is slightly decreased. The most important change upon irradiation was the weakness of the band at 930 cm^{-1}, related to a rocking vibration of the CH_3 group. However, an overall decrease in the intensity of the Raman bands after processing the sample at 266 nm was evident.

Bleached shellac

Micro-Raman spectra recorded on bleached shellac varnishes after laser irradiation are shown in Fig. 6. Little differences were observed in the Raman spectra of shellac after irradiation at 213 and 266 nm when compared with the non-irradiated varnish (Fig. 6). In the reference sample, more variations are shown after processing at 266 nm. Thus, a band at 1736 cm^{-1}, assigned to the stretching vibration of the C=O bond in an ester group appeared, which suggest an esterification process. Besides, the presence of the band at 1474 cm^{-1}, related to vibrations of CH_2/CH_3 is better seen in the spectrum Fig. 6Ac. On the other hand, the previous Raman spectrum showed a decrease in intensity of the bands at 1229, 1086, 1000 and 947 cm^{-1}.These bands are assigned to deformations of CCH, stretching of C-C, deformations of C-C rings and rocking of CH_3, respectively.

Regarding the artificially aged samples, more differences were observed in the Raman spectrum registered after irradiation at 213 nm compared to the other spectra. In particular, the band at 1706

cm^{-1}, assigned to a stretching of the C=O band, is better defined. Besides, an increase of the bands at 1371, 1326, 1266 and 1000 cm^{-1} was also observed. The first two bands are assigned to bending of CH$_2$/CH$_3$, and the third one to bending of CCH and in-plane of =C-H.
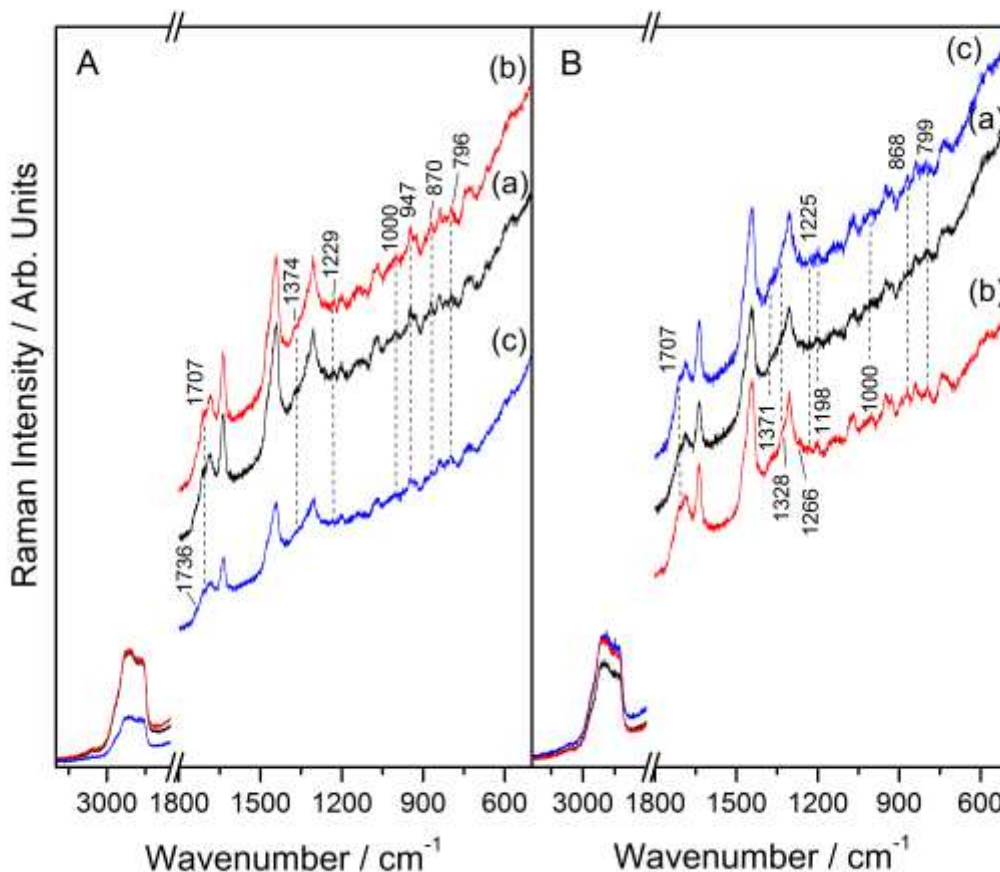

Figure 6 Micro-Raman spectra of reference (A) and artificially aged (B) bleached shellac: non-irradiated sample (a), irradiated at 213 (b) and 266 nm (c).

Finally, the last band corresponds to a deformation of the C-C ring. On the other hand, the Raman spectrum of the sample after irradiation at 266 nm showed an increase of the band at 1225 cm^{-1}, associated with the bending vibration of the CCH group. The Raman spectra of the aged bleached shellac (Fig 6B) did not show
any indication of an esterification reaction, unlike the reference samples. In this case, a cross-linking polymerization could happen.

3.2.4 Characterization of laser irradiation effects by Laser Induced Fluorescence

Chemical modification induced by laser irradiation on varnish samples were also assessed by collecting fluorescence spectra on scanned areas irradiated with 1, 5 and 10 laser pulses. For comparison, the fluorescence maxima (λ_{max}) after normalization were plotted as function of the number of pulses. Results obtained are displayed in Fig. 7.
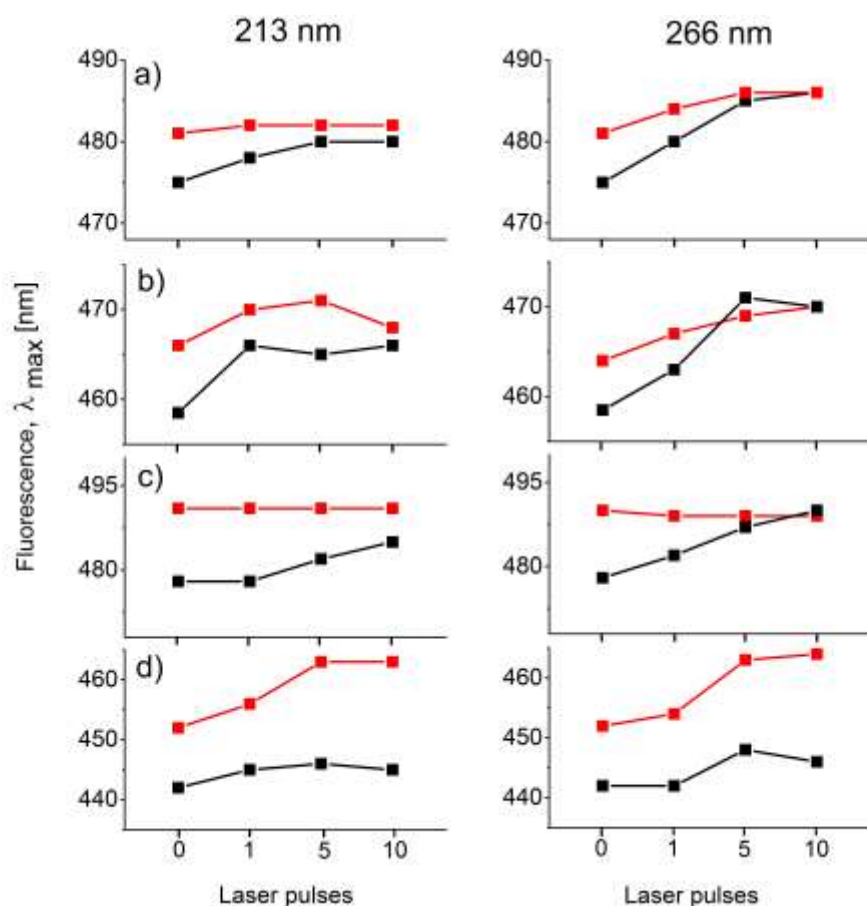
Figure 7 Fluorescence maxima as function of the number of laser pulses after irradiation at 213 nm and 266 nm of mastic a), dammar b), oil-mastic c) and bleached shellac d). Black and red lines correspond to reference and artificially aged samples, respectively.

Basically, reference mastic, dammar and oil mastic samples irradiated at 213 nm showed red-shifts of λ_{max}, which tend to be closer to those of the artificially aged ones, especially after ten pulses. The red shift was less pronounced in reference samples of bleached shellac. However, the λ_{max} shifts of reference samples reached slightly higher values upon irradiation at 266 nm. As regards the fluorescence intensity (data not shown), irradiation at 213 nm of reference mastic and dammar lead to an overall decrease, and the opposite effect in oil mastic. Changes of fluorescence intensity for shellac were instead quite negligible. Contrarily to irradiation at 213 nm, LIF spectra of reference samples irradiated at 266 nm experienced a notable increase of the fluorescence intensity.

Similarly, results from artificially aged mastic and dammar samples displayed a red-shift of λ_{max} although in less extent in comparison to reference samples and more marked at 266 nm. For aged bleached shellac λ_{max} shifts were instead the highest among the investigated samples at both irradiation wavelengths. It is worth noting that λ_{max} of oil mastic did not undergo any shift.

The fluorescence intensity of artificially aged mastic and dammar was reduced at 213 nm while for bleached shellac did not change significantly. Irradiation at 266 nm of the same samples follows a similar quenching behavior although the spectral changes were drastically magnified. Changes observed in shellac resemble those observed upon irradiation at 213 nm. As regards aged oil mastic, irradiation at 213 and 266 nm results in the increase of fluorescence intensity.

4 Discussion

According to the irradiation wavelength, the considered varnish and its degree of oxidation/ polymerization, distinct phenomena occur upon laser irradiation at 213 and 266 nm. Preliminary results obtained from UV-Vis absorption spectroscopy and ablation thresholds, allowed deriving linear absorption coefficient of the studied varnishes, as well as the consideration of the underlying ablation mechanisms. In turn, microscopic examination, micro-Raman and laser induced fluorescence spectroscopy measurements, performed on irradiated areas with fluences two times higher than the single-pulse ablation threshold ($2F_{th}$), have provided the basis for the discussion of the chemical and physical modifications induced by laser irradiation.

As regards the UV-Vis spectral features, the analyzed terpenoid varnishes, with exception of shellac, have the absorption maximum in the far UV. On the other hand, triterpenoid resins mainly consist of polycyclic saturated molecules with dammarane, oleanane, ursane skeletons, which absorb mainly, due to $\pi \rightarrow \pi^*$ electronic transitions, in the 180-190 nm region. Within the investigated range (200-400 nm), reference dammar and mastic films showed a weak shoulder at 230-240 nm ascribable to α,β-unsaturated ketones. The latter were undetected in artificially aged triterpenoids as consequence of the cleavage of keto-group via Norrish type reactions leading to functional groups (i.e. carboxylic groups, aldehydes, and hydroperoxides) with absorption maxima close to 200 nm. As described in section 3.1.1, the maximum absorption in shellac is assigned to α, β-olefinic carboxyl chromophore with a clear UV absorption in the 220-230 region [31, 32].

As expected, the linear absorption coefficients derived for all the varnish samples are significantly higher, from 3 up to 6 times, at 213 with respect to 266 nm and are consistent with the calculated single-pulse F_{th} range. The operating fluences for irradiation at 213 nm of reference and aged samples are nominally rather similar, thus allowing, independently from the varnish degradation, the processing of different terpenoid varnish types with only one wavelength. Most importantly, single-pulse F_{th} found at 213 nm are three times lower than those needed for the discoloration of naturally aged (after eight years) vermilion-based tempera paint, which is known as the most laser sensitive pigment at all tested wavelengths [27]. Instead, the value of F_{th} at 266 nm, depends on the type of varnish, less from the ageing and during the removal, due to the lower absorption, discoloration of the paint layers underneath may easily take place.

Accordingly, RM and ESEM inspections on laser-scanned areas at both wavelengths revealed noticeable morphological differences. Varnish films ablated at 266 nm appear swelled and formation of microsized bubble-like structures (10-15 μm) is detected within the irradiated bulk, as consequence of photo-thermal decomposition. In the literature, it was widely demonstrated that nanosecond UV ablation of weakly absorbing polymers ($\alpha < 1000$ cm^{-1} at the irradiation wavelength) reveals features of a first-order phase transition within the bulk material, bulk boiling, with bubbles formation [46-51]. Formation of a foamy layer was also observed in films of shellac varnish applied on tempera paints upon femtosecond laser irradiation at 795, 398 and 265 nm [27]. Furthermore, as evidenced by Rebollar [52], bubbles growth larger, independently from the value of the linear absorption coefficients (α), in polymers with low molecular weight. It is also observed that the bubble diameter increases with laser fluence above the polymer ablation threshold until a maximum value is reached. Generally the latter is comparable to the optical penetration depth.

The mentioned morphological changes fit well with what is observed herein and are indicative of an ablation mechanism mainly driven by photo-thermal bond-breaking through the ejection of gaseous products. Using laser pulses of 15 ns the thermal diffusion length $z_{th} = 2(D_{th} \cdot \tau)^{1/2}$, where D_{th} is the thermal diffusivity and τ the pulse duration, spans between 77.5 and 24.5 nm

($D_{th} \sim 10^{-3}$–10^{-4} cm^2/s). Although for organic substrates z_{th} is much lower than the optical penetration depth ($1/\alpha$), for a weakly absorbing material, as terpenoid varnishes at 266 nm, the thermal damages may be extended to underlying paint layers.

In contrast ablation at 213 nm, which is a strongly absorbed wavelength, does not results in such deleterious effects (whitish appearance, bubbles) to the etched substrate, which remains morphologically undamaged. In this case, material removal occurs efficiently via purely non-thermal laser ablation (i.e. photochemical) mechanism, with minimal heat diffusion and light penetration to the remaining varnish substrate.

The heat confinement condition ($z_{th} \ll \delta$) allows calculating the depth distribution of the temperature rise as $\Delta T(z) = F_a \cdot e^{-z/\delta}/ \delta \rho C_p$, where ρ is the density and C_p the specific heat of the varnish layer. Here, to estimate the temperature rise attained upon UV laser irradiation, specific heat capacities (C_i) were calculated by using a commercial computational analysis software (PerkinElmer-ChemOffice).

Considering the contribution of the main hydrocarbon skeleton types, the estimated average specific heat capacities are 1.34 and 1.22 J/g·K for triterpenoid (i.e. mastic and dammar), and shellac resins, respectively. Possible contributions arising from different substituent and oxidized groups were not taken into account in this simulation, although they are not expected to give a significant influence. In fact, the monomer molecular weight extrapolated from these calculations is only slightly lower, but of the same order of magnitude, than those measured using different mass spectrometry techniques [53]. The temperature rise at the surface ($z=0$) calculated for single-pulse at F_{th} of reference mastic, dammar and shellac correspond to 150, 120 and 280 °C at 213 nm and to 180, 110 and 500 °C at 266 nm, respectively.

Despite the attained heating may be apparently high, for short laser pulses, the thermal diffusion time $t_{th} = 1/\alpha^2 \cdot D_{th}$ is estimated in 0.1-2 ms at 213 nm and 10-100 ms at 266 nm. This implies that the thermal degradation rate is several orders of magnitude slower than the decomposition and material removal rate, which occurs on a very fast time scale ($\approx$ 30-50 ns). In these conditions, heat diffusion to the substrate is minimal upon laser removal treatment and any thermal side effect is confined within the ablated volume. However, for irradiation tests performed at 266 nm at $2F_{th}$ and successive laser pulses (10 Hz), a possible contribution from incubation effects has to be taken into account.

To assess the maximum extent of chemical changes induced and to get more insight on the ablation mechanisms, Raman measurements were carried out on irradiated areas with $2F_{th}$ and 10 laser pulses delivered on each location. Basically, the spectroscopic data obtained on reference and aged samples are complex and hence, for completeness, they have to be discussed on the basis of the varnish preparation procedure and composition. Thus, reference mastic and dammar have shown, mainly at 213 nm, increase of C=C, C=O, CH$_3$ and CH$_2$ groups and other minor bands accompanied at both wavelengths by a slight red-shift of fluorescence maxima, thus indicating oxidation processes and formation of new chromophores. Irradiation at 266 nm produced Raman spectrum apparently identical to that of the non-treated sample although some bands related to CH$_2$/CH$_3$ and of the C-C-O groups decreased. At the same time red-shift of fluorescence maxima was slightly higher than 213 nm. On the opposite, fluorescence intensity decreased after irradiation at 213 nm while notably increases at 266 nm.

Considering the changes occurring between non-irradiated reference and aged samples (sec. 3.1.2), we can expect that the results obtained on laser irradiated reference samples, especially those following upon irradiation at 213 nm, should be related more to the onset of a stepped oxidation/cross-

linking across the varnish thickness than to laser-induced modifications. As reported in the literature [3,4], oxidation/cross-linking processes in mastic and dammar take place mainly in the uppermost varnish layer. However, it is not to be excluded, as demonstrated by studies conducted on polymers [50, 51], that the absorption of UV light leads also to formation of polar products, including aldehydes, carboxylic acids, esters, methyl and methylene radicals and unsaturated fragments containing C=C bonds. In any way, oxidation gradient and formation of photoproducts may be competitive during the UV laser removal of mastic and dammar varnishes.

Results obtained on artificially aged mastic and dammar films indicate an opposite trend in comparison to reference samples. Here, in contrast to reference samples even less differences are found as well as in the shifts of fluorescence, behavior which has to be mostly correlated to the major extent of photo-oxidative products throughout the film. However, as in the reference sample, increase of C=C, CCH and CH_3 bonds were observed after irradiation at 213 nm. Contrarily, irradiation at 266 nm does not show similar differences although the shoulder bands related to C=O stretching decreased upon irradiation at 266 nm.

The laser treatments applied to the oil-mastic induced very little variations among the Raman spectra. Nevertheless, as previously mentioned for mastic and dammar, small decrease of the bands related to C=O and C=C is shown upon irradiation at 266 nm. These samples can be considered highly oxidized after the thermal treatment and curing procedures and hence, at this wavelength, the loss of these spectral features could be therefore ascribed to an ablation mechanism driven by a photo-thermal process consisting in emission of small fragments and gaseous products (RCH_2OH, CH_3, CH_2, COOH, RCOOR, CO and CO_2). The same consideration cannot be made among the Raman spectra of the aged oil-mastic samples due to the low intensity of the bands.

No evidence of such chemical alteration were pointed out upon irradiation at 213 nm. On the other hand, in varnish films oxidized/ polymerized throughout ablation at 213 nm proceeds by photochemical ablation and hence, without inducing such an effect.

Finally, little differences were observed in the Raman spectra of shellac after treatment at 213 and 266 nm, thus indicating a varnish composition more stable upon laser irradiation. In the reference sample, more variations are shown after processing at 266 nm. Thus, a band at 1736 cm^{-1}, assigned to the stretching vibration of the C=O bond in an ester group appears, which suggest an esterification process.

Regarding the artificially aged samples, more differences are observed in the Raman spectrum registered upon irradiation at 213 nm in comparison to 266 nm. However, the Raman spectra of the aged bleached shellac do not show any indication of an esterification reaction, unlike the reference samples, and the fluorescence maxima tend to be always shifted toward longer wavelength.

5 Conclusions

In this work, UV laser ablation along with associated chemical and physical side effects induced of a set of naturally cured and artificially aged varnishes (mastic, oil mastic, dammar and bleached shellac) were thoroughly characterized using micro-Raman spectroscopy, LIF and ESEM microscopy. In particular, we studied the ablation phenomenology of the fourth (266 nm) and fifth (213) harmonic of the Nd: YAG laser.

The mentioned techniques allowed characterizing both structural differences between unaged and artificially aged samples and the effects associated with the present UV laser ablation. We found the latter strongly depends on the specific UV wavelength, varnish, preparation procedure and the degree

of oxidation/cross linking across the film thickness. The mentioned analytical approach allowed demonstrating that in contrast to the unacceptable modifications induced at 266 nm, minimal chemical changes and the clean surface morphology (no whitish appearance, nor surface damage at micrometer scale) were achieved at 213 nm. The latter exhibited a narrow operating fluence range for the different varnishes and a very controllable micrometric removal, which makes this wavelength very promising for practical applications in painting conservation treatments.

References

[1]   P. Dietemann, C. Higgitt, M. Kälin, M.J. Edelmann, R. Knochenmuss, R. Zenobi, Aging and yellowing of triterpenoid resin varnishes - Influence of aging conditions and resin composition, J. Cult. Herit. 10 (2009) 30–40. doi:10.1016/j.culher.2008.04.007.

[2]   E.R. De La Rie, Old master paintings: a study of the varnish problem, Anal. Chem. 61 (1989) 1228A–1237A. doi:10.1021/ac00196a003.

[3]   C. Theodorakopoulos, V. Zafiropulos, J.J. Boon, S.C. Boyatzis, Spectroscopic investigations on the depth-dependent degradation gradients of aged triterpenoid varnishes, Appl. Spectrosc. 61 (2007) 1045–1051. doi:10.1366/000370207782217833.

[4]   C. Theodorakopoulos, V. Zafiropulos, Uncovering of scalar oxidation within naturally aged varnish layers, J. Cult. Herit. 4 (2003) 216–222. doi:10.1016/S1296-2074(02)01200-1.

[5]   R. Salimbeni, R. Pini, S. Siano, G. Calcagno, Assessment of the state of conservation of stone artworks after laser cleaning: comparison with conventional cleaning results on a two-decade follow up, J. Cult. Herit. 1 (2000) 385–391. doi:10.1016/S1296-2074(00)01094-3.

[6]   S. Siano, R. Salimbeni, Advances in laser cleaning of artwork and objects of historical interest: The optimized pulse duration approach, Acc. Chem. Res. 43 (2010) 739–750. doi:10.1021/ar900190f.

[7]   P. Pouli, M. Oujja, M. Castillejo, Practical issues in laser cleaning of stone and painted artefacts: optimisation procedures and side effects, Appl. Phys. A. 106 (2012) 447–464. doi:10.1007/s00339-011-6696-2.

[8]   L. Carlyle, Laser interactions with paintings: results and proposals for further study. Unpublished Report, The Canadian Conservation Institute, Ottawa, Canada (1981).

[9]   E. I. Hontzopoulos, C. Fotakis, M. Doulgeridis, Excimer laser in art restoration. In: Ninth International Symposium on Gas Flow and Chemical Lasers. Bellingham: SPIE - International Society for Optics and Photonics (1993) pp. 748-751.

[10]   I. Zergioti, A. Petrakis, V. Zafiropulos, C. Fotakis, A. Fostiridou, M. Doulgeridis, Laser applications in painting conservation, in: Lacona I - lasers in the conservation of artworks, Mayer & Comp (1997).

[11]   R. Salimbeni, P. Mazzinghi, R. Pini, S. Siano, M. Vannini, M. Matteini, A. Aldrovandi, Laser restoration of paintings: issues and perspectives, in: Proceedings of the Congress on Science and Technology for the safeguard of Cultural Heritage in the Mediterranean Basi, A. Guarino et al.(Eds.), CNR, Roma (1998)

[12]   S. Georgiou, V. Zafiropulos, D. Anglos, C. Balas, V. Tornari, C. Fotakis, Excimer laser restoration of painted artworks: procedures, mechanisms and effects, Appl. Surf. Sci. 127-129 (1998) 738–745. doi:10.1016/S0169-4332(97)00734-4.

[13]   M. Castillejo, M. Martín, M. Oujja, J. Santamaría, D. Silva, R. Torres, et al., Evaluation of the chemical and physical changes induced by KrF laser irradiation of tempera paints, J. Cult. Herit. 4 (2003) 257–263. doi:10.1016/S1296-2074(02)01143-3.

[14]   R. Teule, H. Scholten, O.F. van den Brink, R.M. a. Heeren, V. Zafiropulos, R. Hesterman, et al., Controlled UV laser cleaning of painted artworks: a systematic effect study on egg tempera paint samples, J. Cult. Herit. 4 (2003) 209–215. doi:10.1016/S1296-2074(02)01137-8.

[15]   M. Castillejo, M. Martín, M. Oujja, D. Silva, R. Torres, A. Manousaki, H. Gouveia Analytical study of the chemical and physical changes induced by KrF laser cleaning of tempera paints. Anal. Chem. 74 (18) (2002) 4662-4671. doi: 10.1021/ac025778c

[16]   M. Wolbarsht, A. de Cruz, Method for cleaning artwork. US Patent, 5,951,778 (1990)

[17]   A. Sansonetti, M. Realini, Nd: YAG laser effects on inorganic pigments. J. Cult. Herit. 1 (2000) 189-198. doi:10.1016/S1296-2074(00)00181-3

[18]   P. Pouli, D.C. Emmony, C.E. Madden, I. Sutherland, Studies towards a thorough understanding of the laser-induced discoloration mechanisms of medieval pigments, J. Cult. Herit. 4 (2003) 271–275. doi:10.1016/S1296-2074(02)01207-4.

[19]   M. Chappé, J. Hildenhagen, K. Dickmann, M. Bredol, Laser irradiation of medieval pigments at IR, VIS and UV wavelengths, J. Cult. Herit. 4 (2003) 264–270. doi:10.1016/S1296-2074(02)01206-2.

[20]   J. Hildenhagen, K. Dickmann, Nd:YAG laser with wavelengths from IR to UV (ω, 2ω, 3ω, 4ω) and corresponding applications in conservation of various artworks, J. Cult. Herit. 4 (2003) 174–178. doi:10.1016/S1296-2074(02)01194-9.

[21]   M. Oujja, M. Sanz, E. Rebollar, J.F. Marco, C. Domingo, P. Pouli, et al., Wavelength and pulse duration effects on laser induced changes on raw pigments used in paintings, Spectrochim. Acta Part A Mol. Biomol. Spectrosc. 102 (2013) 7–14. doi:10.1016/j.saa.2012.10.001.

[22]   S. Siano, J. Agresti, I. Cacciari, D. Ciofini, M. Mascalchi, I. Osticioli, et al., Laser cleaning in conservation of stone, metal, and painted artifacts: State of the art and new insights on the use of the Nd:YAG lasers, Appl. Phys. A Mater. Sci. Process. 106 (2012) 419–446. doi:10.1007/s00339-011-6690-8.

[23]   D. Ciofini, I. Osticioli, a. Pavia, S. Siano, Removal of overpaintings from easel paintings using LQS Nd:YAG laser, Appl. Phys. A. 117 (2014) 341–346. doi:10.1007/s00339-014-8318-2.

[24]   S. Siano, I. Osticioli, A. Pavia, D. Ciofini, Removal of overpaintings from easel paintings using LQS Nd:YAG laser: the first validation study, Stud. Conserv. 60 (2015) (S1), S49-S57. doi: 10.1179/0039363015Z.000000000207

[25]   P. Pouli, A. Selimis, S. Georgiou, C. Fotakis, Recent Studies of Laser Science in Paintings Conservation and Research, Acc. Chem. Res. 43 (2010) 771–781. doi:Doi 10.1021/Ar900224n.

[26]   P. Pouli, I.A. Paun, G. Bounos, S. Georgiou, C. Fotakis, The potential of UV femtosecond laser ablation for varnish removal in the restoration of painted works of art, Appl. Surf. Sci. (2008). doi:10.1016/j.apsusc.2008.04.106.

[27]   M. Oujja, A. García, C. Romero, J.R. Vázquez de Aldana, P. Moreno, M. Castillejo, UV laser removal of varnish on tempera paints with nanosecond and femtosecond pulses., Phys. Chem. Chem. Phys. 13 (2011) 4625–4631. doi:10.1039/c0cp02147d.

[28]   C. V. Horie, Materials for conservation: organic consolidants, adhesives, and coatings. Butterworth-Heinemann series in conservation and museology, Oxford, Boston, 1987.

[29]   M.J. Liu, Simple technique for measurements of pulsed Gaussian-beam spot sizes, Opt. Lett. 7 (1982) 196–198. doi:10.1364/OL.7.000196.

[30]   M. Oujja, P. Pouli, C. Domingo, C. Fotakis, M. Castillejo, Analytical spectroscopic investigation of wavelength and pulse duration effects on laser-induced changes of egg-yolk-based tempera paints, Appl. Spectrosc. 64 (2010) 528–536. doi:10.1366/000370210791211628.

[31]   S. K. Sharma, S. K. Shukla, D. N. Vaid, Shellac-structure, characteristics & modification. Defence Sci. J, 33(3) (1983) 261-271.

[32]   A. B. Upadhye, M. S. Wadia, V. V. Mhaskar, S. Dev, Chemistry of lac resin—IV: Pure lac resin—1: Isolation and quantitative determination of constituent acids. Tetrahedron, 26 (1970) 4177-4187.

[33]   M. S. Wadia, V. V. Mhaskar, S. Dev, On the constitution of Jalaric acid. Tetrahedron Letters, 4 (1963) 513-517.

[34]   M. S. Wadia, R. G. Khurana, V. V. Mhaskar, S. Dev, Chemistry of lac resin - I: Lac acids (part 1): Butolic, jalaric and laksholic acids. Tetrahedron, 25 (1969) 3841-3853.

[35]   R. Knochenmuss, S. Wu, M.J. Dale, R. Zenobi, A Graphite-Assisted Laser Desorption / Ionization Study of Light-Induced Aging in Triterpene Dammar and Mastic Varnishes, 70 (1998) 707–715.

[36]   P. Vandenabeele, B. Wehling, L. Moens, H. Edwards, M. De Reu, G. Van Hooydonk, Analysis with micro-Raman spectroscopy of natural organic binding media and varnishes used in art, Anal. Chim. Acta. 407 (2000) 261–274. doi:10.1016/S0003-2670(99)00827-2.

[37]   H.G.M. Edwards, D.W. Farwell, L. Daffner, Fourier-transform Raman spectroscopic study of natural waxes and resins. I, Spectrochim. Acta - Part A Mol. Spectrosc. 52 (1996) 1639–1648. doi:10.1016/0584-8539(96)01730-8.

[38]   R.H. Brody, H.G.M. Edwards, a. M. Pollard, Fourier transform-Raman spectroscopic study of natural resins of archaeological interest, Biopolym. - Biospectroscopy Sect. 67 (2002) 129–141. doi:10.1002/bip.10059.

[39]   M.M.L. Yu, H.G. Schulze, R. Jetter, M.W. Blades, R.F.B. Turner, Raman microspectroscopic analysis of triterpenoids found in plant cuticles, Appl. Spectrosc. 61 (2007) 32–37. doi:10.1366/000370207779701352.

[40]   A. Nevin, D. Comelli, I. Osticioli, L. Toniolo, G. Valentini, R. Cubeddu, Assessment of the ageing of triterpenoid paint varnishes using fluorescence, Raman and FTIR spectroscopy, Anal. Bioanal. Chem. 395 (2009) 2139–2149. doi:10.1007/s00216-009-3005-4.

[41]   A. Nevin, D. Comelli, I. Osticioli, G. Filippidis, K. Melessanaki, G. Valentini, et al., Multi-photon excitation fluorescence and third-harmonic generation microscopy measurements combined with confocal Raman microscopy for the analysis of layered samples of varnished oil films, Appl. Phys. A Mater. Sci. Process. 100 (2010) 599–606. doi:10.1007/s00339-010-5644-x.

[42]   C. Daher, C. Paris, A.-S. Le Hô, L. Bellot-Gurlet, J.-P. Échard, A joint use of Raman and infrared spectroscopies for the identification of natural organic media used in ancient varnishes, J. Raman Spectrosc. 41 (2010) 1494–1499. doi:10.1002/jrs.2693.

[43]   D. Daferera, C. Pappas, P. A. Tarantilis, M. Polissiou, Quantitative analysis of α-pinene and β-myrcene in mastic gum oil using FT-Raman spectroscopy. Food Chem. 77(4) (2002) 511-515.

[44]   A. Nevin, D. Comelli, G. Valentini, R. Cubeddu, Total synchronous fluorescence spectroscopy combined with multivariate analysis: Method for the classification of selected resins, oils, and protein-based media used in paintings, Anal. Chem. 81 (2009) 1784–1791. doi:10.1021/ac8019152.

[45]   A. Nevin, J.P. Echard, M. Thoury, D. Comelli, G. Valentini, R. Cubeddu, Excitation emission and time-resolved fluorescence spectroscopy of selected varnishes used in historical musical instruments, Talanta. 80 (2009) 286–293. doi:10.1016/j.talanta.2009.06.063.

[46]   Dieter W. Bäuerle, Laser Processing and Chemistry, 2011. doi:10.1524/zpch.1999.208.Part_1_2.291a.

[47]   P.E. Dyer, R. Srinivasan, Nanosecond photoacoustic studies on ultraviolet laser ablation of organic polymers, Appl. Phys. Lett. 48 (1986) 445–447. doi:10.1063/1.96526.

[48]   R. Srinivasan, B. Braren, R. W. Dreyfus, L. Hadel, D. E. Seeger, Mechanism of the ultraviolet laser ablation of polymethyl methacrylate at 193 and 248 nm: laser-induced fluorescence analysis, chemical analysis, and doping studies. JOSA B, 3(5) (1986) 785-791.

[49]   N. Bityurin, 8 Studies on laser ablation of polymers, Annu. Reports Sect. "C" (Physical Chem. 101 (2005) 216. doi:10.1039/b408910n.

[50]   T. Lippert, J.T. Dickinson, Chemical and spectroscopic aspects of polymer ablation: Special features and novel directions, Chem. Rev. 103 (2003) 453–485. doi:10.1021/cr010460q.

[51]   E. Rebollar, G. Bounos, M. Oujja, S. Georgiou, M. Castillejo Effect of molecular weight on the morphological modifications induced by UV laser ablation of doped polymers, J. Phys. Chem. B, 110 (33) (2006) 16452-16458. doi: 10.1021/jp062060i

[52]   E. Rebollar, G. Bounos, M.Oujja, C. Domingo, S. Georgiou, M. Castillejo, Influence of polymer molecular weight on the chemical modifications induced by UV laser ablation, J. Phys. Chem. B 110(29) (2006) 14215-14220. doi: 10.1021/jp061451u

[53]   M. P. Colombini, F. Modugno, Organic mass spectrometry in art and archaeology, (Eds.). John Wiley & Sons. (2009).